Tellus (2005), 58B, 88–94
Printed in Singapore. All rights reserved

TELLUS

Tidal influence on the sea-to-air transfer of CH_4 in the coastal ocean

By DOSHIK HAHM, GUEBUEM KIM*, YONG-WOO LEE, SUNGH-YUN NAM, KYUNG-RYUL KIM and KUH KIM, *School of Earth and Environmental Sciences/RIO, Seoul National University, Seoul 151-742, Korea*

(Manuscript received 21 December 2004; in final form 15 August 2005)

ABSTRACT

We obtained real-time monitoring data of water temperature, salinity, wind, current, CH_4 and other oceanographic parameters in a coastal bay in the southern sea of Korea from July 8 to August 15, 2003, using an environmental monitoring buoy. In general, the transfer velocity of environmental gases across the air–sea interface is obtained exclusively from empirical relationships with wind speeds. However, our monitoring data demonstrate that the agitation of the aqueous boundary layer is controlled significantly by tidal turbulence, similar to the control exercised by wind stress in the coastal ocean. The sea-to-air transfer of CH_4 is enhanced significantly during spring tide due to an increase in the gas transfer velocity and vertical CH_4 transport from bottom water to the surface layer. Thus, our unique time-series results imply that the sea-to-air transfer of gases, such as CH_4, DMS, DMHg, N_2O, CO_2 and ^{222}Rn, from highly enriched coastal bottom waters, is controlled not only by episodic wind events but also by regular tidal turbulence in the coastal ocean.

1. Introduction

The flux of environmental gases across the air–sea interface is a function of gas transfer velocity (k) and the concentration difference (ΔC) between the surface-mixed layer and the air–sea boundary layer, where the concentration is in equilibrium with the atmosphere,

$$F = k\Delta C. \quad (1)$$

The transfer of slightly soluble gases is restricted by a thin aqueous boundary layer at the air–sea interface, where molecular diffusion dominates (Jähne and Haußecker, 1998). The magnitude of k is determined by the molecular diffusivity and diffusion through this layer whose thickness is a function of near-surface turbulence. Both boundary layer models and dimensional analyses indicate that an increase in the turbulence level results in a decrease in the thickness of the layer (increase in k).

In addition, the surface renewal model (Danckwerts, 1970), which assumes that the boundary layer is continually replaced with the bulk water below due to turbulent eddies, has been regarded as a useful conceptual model for k. Modern technology facilitates the direct detection of ΔC for most gases comprising the atmosphere in situ; however, it has been difficult to measure k directly in a field. Consequently, the determination of gas flux in the ocean relies on an empirical parametrization of k.

For the open ocean, momentum flux due to wind is considered to be a major parameter responsible for controlling k. It plays a role in triggering other parameters such as the wave field and whitecap coverage, which also causes k to vary (Woolf, 1997; Bock et al., 1999). Several types of relationships between wind speed and gas transfer velocity have been suggested on the basis of a number of independent wind tunnel and field experiments using tracers such as ^{222}Rn, SF_6 and ^3He (for example, Liss and Merlivat, 1986; Wanninkhof, 1992; Wanninkhof and McGillis, 1999).

In estuaries and the coastal ocean, it seems that boundary friction and tide, in addition to wind, play significant roles in generating turbulent energy (Cerco, 1989; MacIntyre et al., 1995; Zappa et al., 2003). Zappa et al. (2003) measured some turbulence-related parameters such as the surface renewal rate and turbulent dissipation rate (ε) using infrared imagery and a high-frequency acoustic Doppler velocimeter. They showed that the parameters correlated closely with tidal speed and k estimated by the gradient flux technique under low wind-speed conditions. Their results demonstrated that the turbulent transport associated with tidal speed is potentially an important factor with respect to the gas exchange in coastal systems.

Therefore, in this study, we measured many water and atmospheric properties including salinity, temperature, current, CH_4 concentration and wind speed by deploying a real-time

*Corresponding author.
e-mail: gkim@snu.ac.kr
DOI: 10.1111/j.1600-0889.2005.00170.x

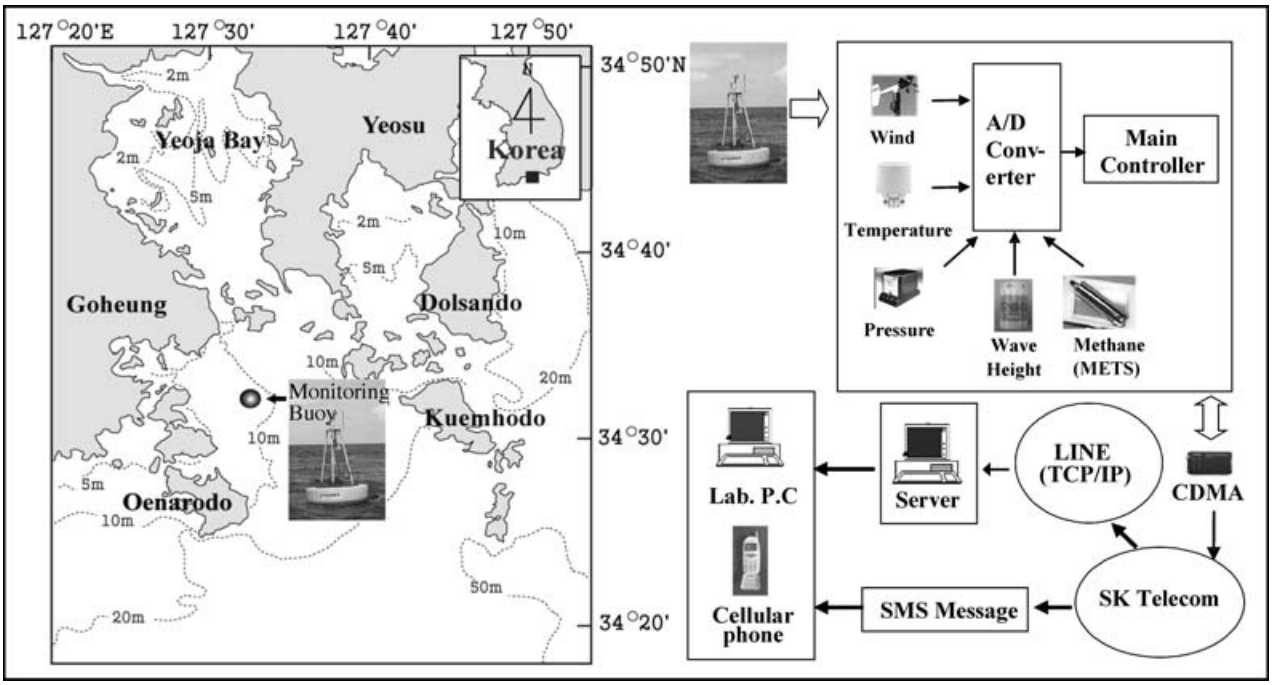

Fig. 1. Schematic view of the real-time monitoring buoy systems at Narodo in the southern sea of Korea.

monitoring buoy in a coastal bay. The 40-d dataset allowed us to determine the influence of tide on near-surface turbulence and the mixing of the water column. We calculated the tide- and wind-driven gas transfer velocities and used them to calculate the sea-to-air fluxes of CH_4, which is one of the gases responsible for regulating the radiation balance and atmospheric chemistry of the Earth.

2. Real-time monitoring buoy

In order to understand real world processes, we require time-series information on physical and biogeochemical variations. Therefore, we developed a monitoring buoy system that houses various environmental sensors for measuring water and air temperature, salinity, wind, current, CH_4 and other oceanographic parameters (Fig. 1). The temperature and salinity of water were measured at three depths (1.7, 5.7 and 7.3 m) using SBE37 conductivity–temperature–depths (CTDs). The water currents through the entire water column were measured using an RDI 300 kHz acoustic Doppler current profiler (ADCP).

The concentration of CH_4 was measured at a distance of 1.5 m from the surface by using a commercial underwater CH_4 sensor (METS by CAPSUM technologie). The measurement principle is that the hydrocarbon molecules diffuse out of the liquid into the detector chamber through a special silicon membrane. The adsorption of hydrocarbons onto the active layer leads to an electron exchange with oxygen and therefore the resistance is varied. This variation is converted into a voltage by the electronic device. The membrane is composed of silicon with a thickness of 10 μm. The detection limit is 20 nmol L^{-1} with a reaction time of 3–30 min. Detailed information on this sensor can be obtained from the manufacturer (http://www.capsum.com). Using this sensor, Kim and Hwang (2002) successfully monitored CH_4 in submarine waters over a period of several months. During their study period, they found that the concentration of CH_4 varied in proportion to that of ^{222}Rn due to fluctuations in the submarine groundwater discharge. This confirms a minimal drifting effect of this sensor in seawater.

We employed code division multiple access (CDMA) as a communication platform for two-way communication between the sensors on the buoy and a database computer and/or personal cellular phone (Nam et al., 2005). The CTD, ADCP and CH_4 sensors were programmed to generate data at 10-min intervals. Simultaneously, meteorological data such as air temperature, pressure, humidity and wind speed were obtained from the buoy. The buoy was deployed at the centre of a bay (9 m in depth) in the southern sea of Korea (34°31′N, 127°32′E) from July 8 to August 15, 2003 (Fig. 1).

3. Results and discussion

Large variations in water temperature and salinity were observed (Fig. 2). The overall trend could be due to changes in solar radiation and rainfall during summer. A pronounced feature of the results is that the salinity and temperature differences between the surface and bottom layers increase at neap tide. This indicates that the tidal force is not sufficiently strong to mix the water

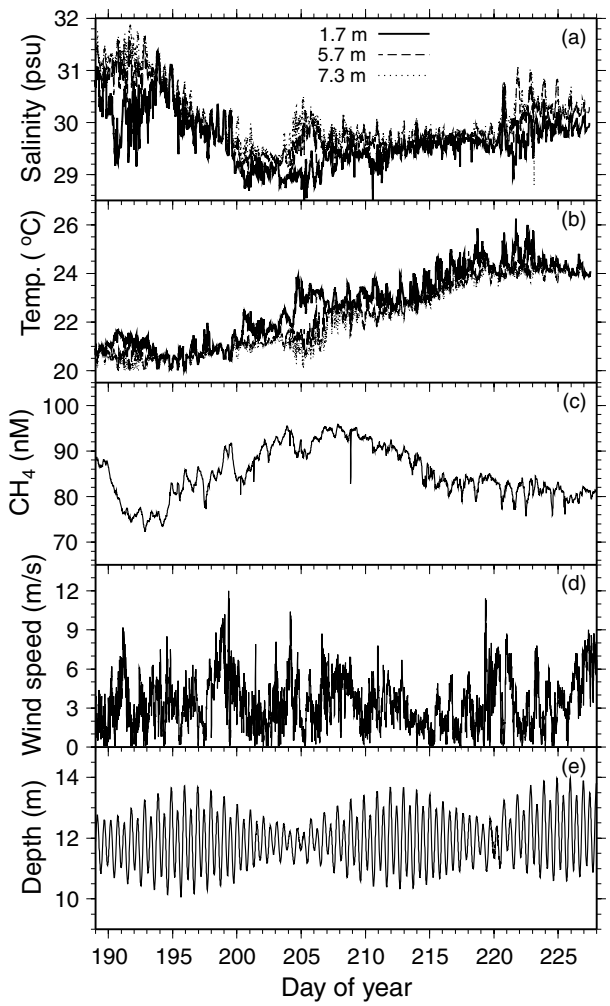

Fig. 2. Temporal variations in the oceanic parameters and CH_4 in seawater in the southern sea of Korea from July 8 to August 15, 2003. (a) The salinity and (b) temperature obtained at three depths, (c) CH_4 in the surface layer, (d) wind speed measured approximately 1.8 m above the sea surface and (e) water depth indicating the tidal cycle.

column at neap tide. The differences were rather small around day 222 when the wind speed was higher than 10 m s^{-1}. It is likely that the wind played a significant role in mixing the water column during that period.

The variation in CH_4 is largely opposite to that in salinity, thereby indicating relatively high concentrations of CH_4 in less saline water. This result may be due to a strong input of CH_4 from the submarine groundwater discharge in Yeoja Bay during a period of high precipitation, as documented by Hwang et al. (2005) by means of Ra tracers. In the following sections, we determine the relative importance of the factors (wind speed versus tidal speed) that control the sea-to-air transfer of CH_4, which, along with biological oxidation, constitutes a major sink in the coastal ocean.

3.1. Gas transfer velocity due to the wind

In order to estimate the gas transfer velocity due to the wind, we employed the relationship for short-term wind speeds given by Wanninkhof (1992):

$$k_{W92} = 0.31 u_{10}^2 (Sc/660)^{-1/2}, \quad (2)$$

where u_{10} is the wind speed at a distance of 10 m above the sea surface and Sc (Schmidt number) is defined as the ratio of water viscosity (ν) to the diffusion coefficient of the gas (D). Since the wind speed sensor of the buoy is located approximately 1.8 m above the sea surface, the measured wind speeds ($u_{1.8}$; Fig. 2d) were converted to u_{10} by using the neutral drag law given by Smith (1988). The Schmidt number of CH_4 was calculated using the relationship derived by Wilke and Chang (1955). During the observation period, the gas transfer velocity due to the wind, k_{W92}, was below 30 cm h^{-1}, with the exception of large peaks reaching 60 cm h^{-1} on days 198 and 218 (Fig. 3a). The gas transfer velocities based on the relationships given by Liss and Merlivat (1986) and Wanninkhof and McGillis (1999) were also calculated in order to compare the resultant difference in the flux (Fig. 3e).

3.2. Gas transfer velocity due to the tide

Lamont and Scott (1970) developed a model based on small-scale motions present in an eddy cell to predict the surface renewal rate. By using this model and the Kovasznay turbulent energy spectrum (Hinze, 1975), they derived the following equation:

$$k_\varepsilon = 0.4(\varepsilon\nu)^{1/4} Sc^{-1/2}, \quad (3)$$

where ε is the turbulent kinetic energy dissipation rate (W kg^{-1}) and ν is the kinematic viscosity of water. Although the value of ε can be calculated from the magnitude of the wave-number spectrum in the inertial subrange (Zappa et al., 2003), our measurement interval of ADCP (10 min) is too long to show the wave-number spectrum in this subrange. Instead, we estimated the dissipation rate in terms of the tidal speed alone by fitting eq. (4) to the results obtained by Zappa et al. (2003). The form of eq. (4) is selected as the best fit among the various functions for the given range,

$$\varepsilon = aV^{1.1/V}, \quad (4)$$

where V is the tidal speed in m s^{-1} and a is a constant of value 1.07×10^{-4}. For this case, the wave-number spectrum in the inertial subrange is assumed to be the same function of the tidal speed at the two regions.

The tidal speed, V, was calculated from the ADCP measurements at each depth level by a two-dimensional vector harmonic analysis (Foreman, 1996) using 38 tidal constituents. The analysis reveals dominant current oscillations in a direction along the bay, with typical magnitudes of 20–30 cm s^{-1} and 10–20 cm s^{-1} at M2 and S2 periods (12.42 and 12.00 hr),

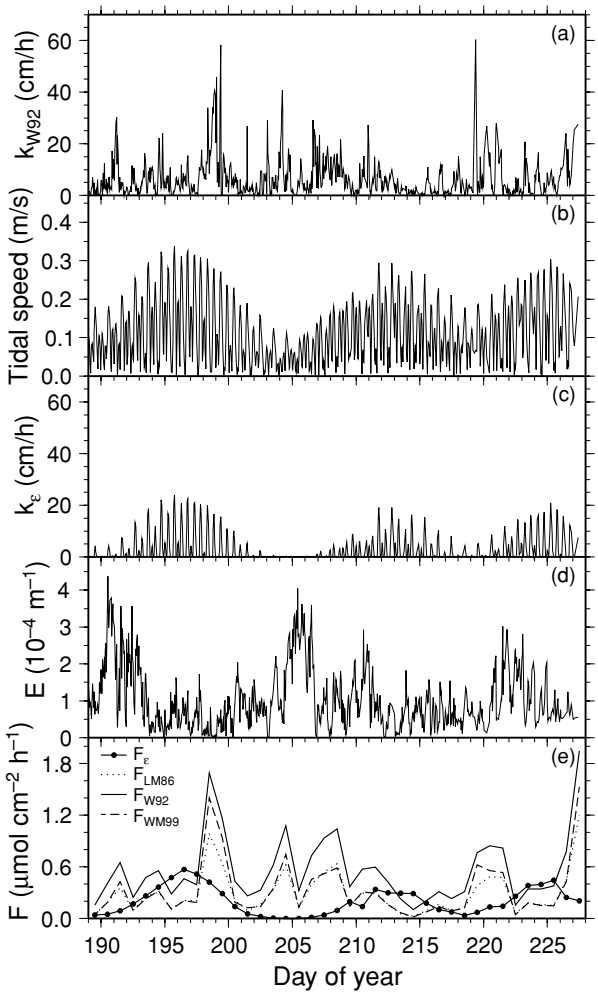

Fig. 3. Temporal variations in the (a) gas transfer velocity due to the wind (k_{W92}), (b) tidal speed, (c) gas transfer velocity due to the tide (k_ε), (d) density gradient (stability) between the depths of 1.7 m and 5.7 m and (e) CH_4 fluxes calculated based on the wind (F_{W92}, F_{LM86} and F_{WM99}) and tide (F_ε).

respectively. The calculated tidal speed exhibits strong semidiurnal oscillations during the periods of days 193–198, 210–215 and 224–229, which are consistent with the oscillations in water depth (Figs 3b and 2e). This indicates that the tidal current is well calculated from the ADCP measurements. The tidal speed was 20–35 cm s^{-1} during spring tide and 5–15 cm s^{-1} during neap tide. The turbulent dissipation rate (ε) was calculated from V (Fig. 3b) and then used to estimate the gas transfer velocity due to the tide (k_ε; eq. 3).

While Zappa et al. (2003) directly correlated the water current measured using the ADCP with ε, we fed the tidal component only into eq. (4). This component was obtained from the ADCP measurements by the two-dimensional harmonic analysis. The purpose was to remove any possible interaction between the wind speed and the tide due to a higher wind variation than that of Zappa et al. (2003). This implicitly assumes that the contributions of the wind (k_{W92}) and tide (k_ε) to the gas transfer are additive (Borges et al., 2004).

In addition to the tidal speed (or stream flow), water depth contributes to the generation of turbulent energy by bottom friction. According to the relationship given by O'Connor and Dobbins (1958), the reaeration coefficient (k_2) is inversely proportional to the 3/2 power of the depth (H). Considering the gas transfer velocity to be the product of k_2 and H, it can be expected that the gas transfer velocity due to the tide would decrease with an increase in the water depth ($k_\varepsilon \propto H^{-1/2}$). The relationship suggests that an increase in the water depth from ~3 m (Zappa et al., 2003) to ~12 m (this study) should result in a 50% decrease in the near-surface turbulence. However, since eq. (4) intrinsically includes the effect of bottom friction, the change in k_ε with an increase in the depth could not be estimated quantitatively in this study. Thus, extensive future studies are required to determine quantitatively the tidal effect on the air–water gas exchange as a function of the water depth in the coastal environment.

3.3. Sea-to-air transfer of CH_4

The gas transfer velocities due to the tide and wind are compared in Fig. 4. Under the condition that the wind speed is below 6 m s^{-1}, the tidal speed higher than 0.25 m s^{-1} accounts for more than half the gas transfer. Since wind speed alone has been used for calculating the gas transfer velocity in the coastal ocean (Corbett et al., 1999; Burnett et al., 2003), our results suggest a new direction for this field requiring further follow-up studies.

The CH_4 fluxes due to the tide (F_ε) and wind (F_{W92}) were independently calculated from the estimated values of k_ε and k_{W92} and the concentration difference (eq. 1) between the surface-mixed layer and the air–sea boundary layer, where the concentration is in equilibrium with the atmosphere. We calculated the equilibrium solubility of CH_4 according to Weisenburg and Guinasso (1979) by assuming an average atmospheric CH_4 concentration of 1.8 ppm (Dlugokencky et al., 1993), which is negligible as compared with our measured concentrations. The air–sea boundary layer may not be in equilibrium with the atmosphere because of microbial consumption. In fact, Upstill-Goddard et al. (2003) argued that bacterioneuston oxidizes CH_4 in this layer and increases its sea-to-air exchange by ~12%. Although microbial consumption can enhance the absolute flux, the relative magnitude of the CH_4 fluxes due to the tide and wind remains valid. The daily averaged fluxes due to the tide (F_ε) and wind (F_{LM86}, F_{W92} and F_{WM99}) are shown in Fig. 3e. Considering that F_{W92} was consistently higher than F_{LM86} and F_{WM99}, F_{W92} should be regarded as an upper limit of the CH_4 flux due to the wind. Although the mean F_{W92} (μmol cm^{-2} h^{-1}) of 0.56 was larger than the mean F_ε of 0.20, the fraction of CH_4 flux (F_ε) due to the tide is generally predominant during spring tides.

The concentration of CH_4 is considerably high in coastal groundwater and bottom water. For example, Bugna et al. (1996) found that the CH_4 concentrations in groundwater and near-shore

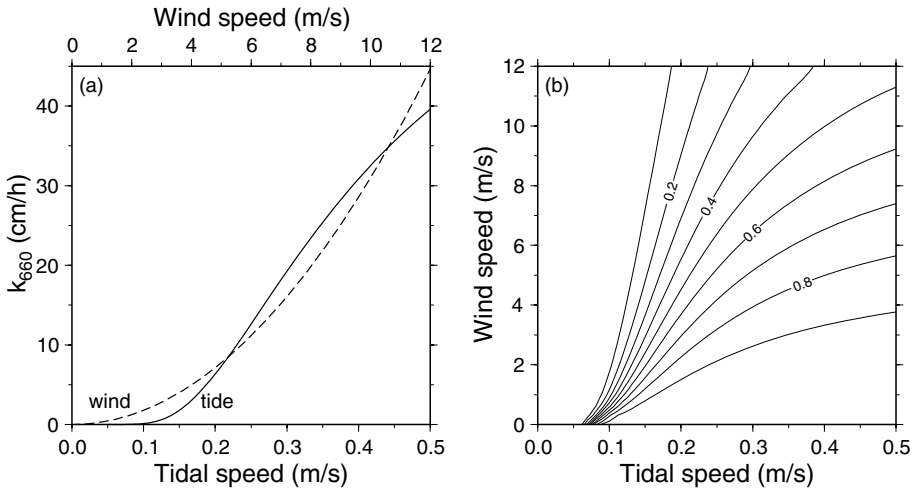

Fig. 4. (a) Dependency of the gas transfer velocities on the wind and tide and (b) the ratio of the gas transfer velocities due to the tide to the sum of the velocities due to the tide and wind ($k_\varepsilon/[k_\varepsilon + k_{W92}]$). k_{660} is the gas transfer velocity for a Schmidt number of 660, the value for CO_2 in seawater at 20°C.

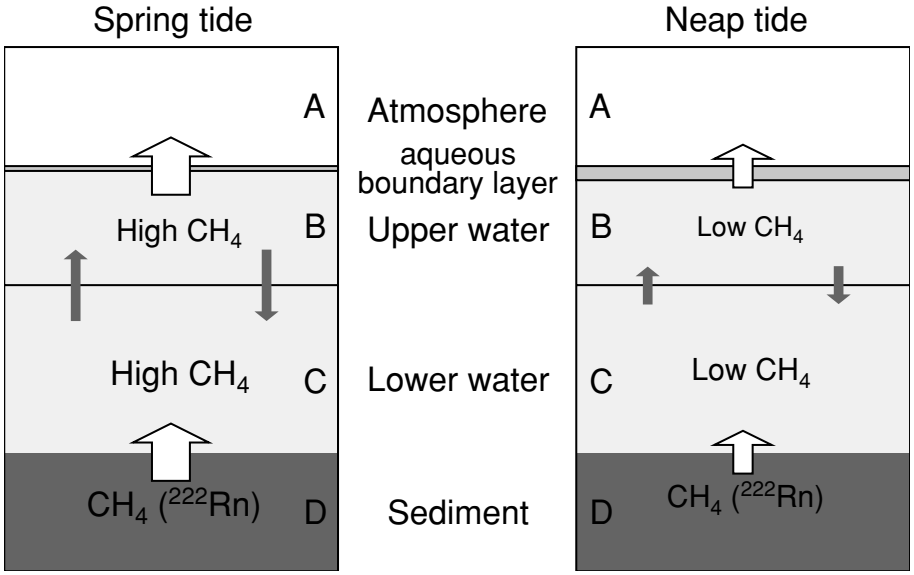

Fig. 5. A hypothesis showing the difference in the fluxes of CH_4 between spring and neap tides in the coastal ocean. Relatively higher fluxes through the boundary layers are expected due to a larger submarine groundwater discharge (CD interface) vertical mixing (BC interface) and a thinner boundary layer (AB interface) during spring tides.

seawater of the Gulf of Mexico were as high as 61 μM and 62 nM, respectively. Thus, in order to investigate the vertical transport of CH_4 from bottom water to the surface layer (eventually controlling ΔC_{CH4} in eq. 1), we calculated the water stability (Knauss, 1997) that is defined as the density gradient between the surface (1.7 m) and below it (5.7 m):

$$E = \frac{1}{\rho}\left(\frac{\partial \rho}{\partial z}\right). \tag{5}$$

The three peaks of stability for the time-series data coincide with neap tides on days 190, 215 and 221 (Fig. 3d). If we consider normal condition of a constant supply of CH_4 from upstream, the CH_4 input to the surface layer will be enhanced due to higher vertical mixing under unstable water column conditions during spring tide.

Furthermore, Kim and Hwang (2002) documented that submarine groundwater discharge, which is one of the main sources of CH_4 in the coastal ocean, is enhanced significantly at spring tide during summer when aquifers are recharged adequately. Similar variations of submarine groundwater discharge, with a semi-monthly period due to neap-spring tidal pumping, were also found independently by automated seepage meters (Taniguchi, 2002).

By combining the overall effects, there are three apparent positive effects on the sea–air gas exchange during spring tide: (1) gas transfer velocity, (2) supply of CH_4 from bottom water to the surface layer and (3) submarine groundwater discharge (Fig. 5). The relative importance of these factors will vary according to hydrogeochemical and oceanographic settings. Therefore, more extensive studies are necessary to include these factors in constraining the sea–air exchange of environmental gases in the coastal ocean.

4. Conclusions

We successfully obtained real-time monitoring data of temperature, salinity, current, CH_4 and wind speed in the southern sea of Korea. Our results reveal that the agitation of the sea surface is controlled mainly by the tidal and wind speeds. This suggests that the sea-to-air transfer of environmental gases increases considerably during spring tide due to an increase in the gas transfer velocity, vertical water mixing and submarine groundwater discharge. Our results imply that the sea-to-air transfer of critical environmental gases (DMS, CH_4, DMHg, ^{222}Rn, CO_2, etc.) is significantly controlled by the tidal turbulence in the coastal ocean, in addition to episodic wind events. For an effective study of the gas exchange in the future, both ^{222}Rn and CH_4 sensors may be included in the monitoring buoy for more depths and stations.

5. Acknowledgments

The authors are grateful to two anonymous reviewers for their constructive comments to improve this manuscript. This study was supported by the Korea Research Foundation Grant funded by the Korean Government (MOEHRO) (R08-2003-000 -10328-0).

References

Bock, E. J., Hara, T., Frew, N. M. and McGillis, W. R. 1999. Relationship between air–sea gas transfer and short wind waves. *J. Geophys. Res.* **104**, 25 821–25 831.

Borges, A. V., Vanderborght, J.-P., Schiettegatte, L.-S., Gazeau, F., Ferron-Smith, S., and co-authors 2004. Variability of the gas transfer velocity of CO_2 in a macrotidal estuary (the Scheldt). *Estuaries* **27**, 593–603.

Bugna, G. C., Chanton, J. P., Cable, J. E., Burnett, W. C. and Cable, P. H. 1996. The importance of groundwater discharge to the methane budgets of nearshore and continental shelf waters of the northeastern Gulf of Mexico. *Geochim. Cosmochim. Acta* **60**, 4735–4746.

Burnett, W. C., Bokuniewicz, H., Huettel, M., Moore, W. S. and Taniguchi, M. 2003. Groundwater and porewater inputs to the coastal zone. *Biogeochem.* **66**, 3–33.

Cerco, C. F. 1989. Estimating estuarine reaeration rates. *J. Environ. Eng.* **115**, 1066–1070.

Corbett, D. R., Chanton, J., Burnett, W., Dillon, K. and Rutkowski, C. 1999. Patterns of groundwater discharge into Florida Bay. *Limnol. Oceanogr.* **44**, 1045–1055.

Danckwerts, P. V. 1970. *Gas–Liquid Reactions*. McGraw-Hill, New York.

Dlugokencky, E. J., Harris, J. M., Chung, Y. S., Tans, P. P. and Fung, I. 1993. The relationship between the methane seasonal cycle and regional sources and sinks at Tae-ahn peninsula, Korea. *Atmos. Environ.* **27A**, 2115–2120.

Foreman, M. G. G. 1996. Manual for tidal current analysis and prediction. In: *Pacific Marine Science Report 786*. Institute of Ocean Science, Sidney, B. C., Canada, pp. 57.

Hinze, J. O. 1975. *Turbulence* 2nd Edition, McGraw-Hill, New York.

Hwang, D. W., Kim, G., Lee, Y. W. and Yang, H. S. 2005. Estimating submarine inputs of groundwater and nutrients to a entropic coastal bay using a radium tracer. *Mar. Chem.* **96**, 61–71.

Jähne, B. and Haußecker, H. 1998. Air–water gas exchange. *Annu. Rev. Fluid Mech.* **30**, 443–468.

Kim, G. and Hwang, D. W. 2002. Tidal pumping of groundwater into the coastal ocean revealed from submarine ^{222}Rn and CH_4 monitoring. *Geophys. Res. Lett.* **29**, doi:10.1029/2002GL015093.

Knauss, J. A. 1997. *Introduction to Physical oceanography* 2nd Edition, Prentice-Hall, New Jersey.

Lamont, J. C. and Scott, D. S. 1970. An eddy cell model of mass transfer into the surface of a turbulent liquid. *AIChE J.* **16**, 513–519.

Liss, P. S. and Merlivat, L. 1986. Air-sea gas exchange rates: introduction and synthesis. In: *The Role of Air–Sea Exchange in Geochemical Cycling* (ed. P. Buat-Menard). D. Reidel, Hingham, Mass, 113–129.

MacIntyre, S., Vera, R. and Chanton, J. P. 1995. Trace gas exchange across the air-water interface in freshwater and coastal marine environments. In: *Biogenic Trace Gases: Measuring Emissions Form Soil and Water* (eds. P. A. Matson and R. C. Harriss), Blackwell Scientific Publishing, Cambridge, Massachusetts, 52–97.

Nam, S.-H., Kim, G., Kim, K.-R., Kim, K., Oh, L., and co-authors. 2005. Application of real-time monitoring buoy systems for physical and biogeochemical parameters in the coastal ocean around the Korean peninsula. *Mar. Tech. Soc. J* **39**, 54–64.

O'Connor, D. and Dobbins, W. 1958. Mechanism of reaeration in natural streams, *Trans. Am. Soc. Civ. Eng.* **123**, 641–684.

Smith, S. D. 1988. Coefficients for sea surface wind stress, heat flux and wind profiles as a function of wind speed and temperature. *J. Geophys. Res.* **93**, 15467–15472.

Taniguchi, M. 2002. Tidal effects on submarine groundwater discharge into the ocean. *Geophys. Res. Lett.* **29**, doi: 10.1029/2002GL014987.

Upstill-Goddard, R. C., Frost, T., Henry, G. R., Franklin, M., Murrell, J. C., and co-authors. 2003. Bacterioneuston control of air–water methane exchange determined with a laboratory gas exchange tank. *Global Biogeochem. Cycles* **17**, 1108, doi: 10.1029/2003GB002043.

Wanninkhof, R. 1992. Relationship between wind speed and gas exchange over the ocean. *J. Geophys. Res.* **97**, 7373–7382.

Wanninkhof, R. and McGillis, W. R. 1999. A cubic relationship between air–sea CO_2 exchange and wind speed. *Geophys. Res. Lett.* **26**, 1889–1892.

Weisenburg, D. A. and Guinasso, N. L. Jr. 1979. Equilibrium solubility of methane, carbon monoxide and hydrogen in water and sea water. *J. Chem. Eng. Data* **24**, 356–360.

Wilke, C. R. and Chang, P. 1955. Correlation of diffusion coefficients in dilute solutions. *AIChE J.* **1**, 264–270.

Woolf, D. K. 1997. Bubbles and their role in gas exchange. In: *The Sea Surface and Global Change* (eds. P. S. Liss and R. A. Duce), Cambridge University Press, Cambridge, 173–205.

Zappa, C. J., Raymond, P. A., Terray, E. A. and McGillis, W. R. 2003. Variation in surface turbulence and the gas transfer velocity over a tidal cycle in a macrotidal estuary. *Estuaries* **26**, 1401–1415.